

Estimation of crop water requirement in rice-wheat system from multi-temporal AWiFS satellite data

Mamta Kumari¹, N. R. Patel², Payshanbe Yaftalov Khayruloevich³

1- Scientist, Agric. & Soils Department, Indian Institute of Remote Sensing, Dehradun, India

2- Scientist, Agric. & Soils Department, Indian Institute of Remote Sensing, Dehradun, India

3- Engineer, State Organization for Hydrometeorology, Dushanbe, Republic of Tajikistan

mamta9507@gmail.com

ABSTRACT

The present study investigates remote sensing based approach of large-area crop water requirement using vegetation indices as proxy indicator of crop coefficient (Kc). This study is an attempt to estimate the reasonably proper Kc for lowland rice and wheat and subsequently crop evapotranspiration (ETc) in rice-wheat system using multitemporal IRS P6-AWiFS data integrated with meteorological data following FAO-56 approach. Geometrically and radiometrically corrected multi-temporal AWiFS images were classified by rule based classifier to discriminate rice-wheat system from other cropping system. Monthly biophysical parameters viz., fractional canopy cover (f_c) and water scalar factor (Ws) were derived from spectral indices in order to adjust Kc for the different growth stages in rice-wheat system. The results showed that after including Ws with f_c for rice, degree of fit (R^2) has been significantly improved from 0.72 to 0.94 for Kc estimation of rice. Satellite derived Kc has captured the effect of phenology and management practices in study area. The estimated crop water requirement was 241.66, 531.34, 440.86 and 192.63 Mha.m for rice and 127.43, 135.77, 305.55, 262.84 and 204.5 Mha.m for wheat at various growth stages.

Keywords: Evapotranspiration, crop coefficient, rice-wheat system, fractional vegetation cover.

1. Introduction

Rice-wheat system is the most important and largest production system in India, occupies 10 million hectares area extending from Indo-Gangetic plain to foothills of Himalayan. Increase in cropped as well as irrigated area coupled with high cropping intensity and a major shift towards rice-wheat culture has led to over-exploitation of groundwater resulting in declining ground water resources. Besides shrinking of water resources, the adoption of input (e.g. irrigation or fertilizer) intensive cultivation has invited many environmental problems viz., waterlogging; salinity; loss of fertilizes; ground water pollution and eutrophication. The rapidly depleting water resources and agro-environmental health threaten the sustenance of existing levels of agricultural production, and call for efficient use of water over space and time. The best applicable strategy to optimize water use on large scale is achieved through spatially explicit and accurate estimates of crop water demand and supply in a region. Over last two decades, considerable progresses have been made to understand key factors controlling crop water requirement and consequently led to development of new techniques of evapotranspiration (ET) estimation (Patel *et al.* 2005) but operational applications of ET estimates yet heavily rely on the FAO-56 model because of minimum requirement of phenological and standard meteorological inputs (Evelt *et al.* 1995; Kite and Droogers 2000;

Allen 2000; Eitzinger *et al.* 2002). In FAO-56 approach, actual ET is calculated by combining reference evapotranspiration (ET_0) and K_c . Although many work has been done to estimate K_c experimentally for many crops (Doorenbos and Pruitt 1977; Snyder *et al.* 1987; Jensen *et al.*, 1990; Allen *et al.* 1998), it is very difficult to capture spatial heterogeneity in K_c due to its dependence on climate, soil type, crop type and its varieties and varying management inputs e.g. irrigation technique, soil moisture, nutrient availability and plant phenology (Allen *et al.* 1998). Therefore, specific adjustment of crop coefficients in various climatic regions is essential.

The spectral measurement can resolve this issue as K_c and vegetation indices (VIs) are sensitive to dynamics of crop cover i.e., leaf area index and fractional ground cover (Heilman *et al.* 1982; Jackson and Huete 1992; Choudhury *et al.* 1994; Moran *et al.* 1995). Satellite remote sensing gives the opportunity to monitor the space and time variability of vegetation phenology (Baret and Guyot 1991; Hall *et al.* 1995; Carlson and Ripley 1997; Myneni *et al.* 1997; Duchemin *et al.* 1999; Gutman 1999; Bastiaanssen *et al.* 2000) which makes it very important tool to estimate surrogate K_c based on VIs. The remotely sensed K_c responds to actual crop condition that varies from field to field and captures the variability in K_c that occurs due to management soil conditions. Many studies have been done to estimate K_c from VIs at field and regional scales (Rouse *et al.* 1974; Jackson *et al.* 1980; Huete 1988; Bausch and Neale 1987; Choudhury *et al.* 1994; Bausch 1995; Ray and Dadhwal 2001; Duchemin *et al.*, 2002) and showed the similarity in the seasonal pattern of K_c and VI.

Mishra *et al.* (2005) estimated crop coefficients of paddy crop grown in irrigation command using remote sensing data; however, the impounded water background in paddy fields might have influenced the crop reflectance and affected the results to a great extent. The unique spectral feature of paddy field during transplanting season underestimates the Normalized Difference Vegetation Index (NDVI) and consequently affects the K_c estimation. Most of K_c estimation related work through satellite data has been done in crops e.g. wheat, corn etc which are not affected by water background. Standard K_c curve of rice in particular differs from other crops and as a result the NDVI based measure of K_c could be erroneous since NDVI cannot capture contribution of impounded water content to K_c . The standard K_c curve of paddy in general has higher magnitude of K_c at initial stage despite of negligible canopy cover due to the contribution of impounded water during early phase. Moreover, an NDVI values are negative in water impounded condition and so underestimates K_c value during early phase.

The water sensitive indices which take both vegetation and water background effect into the account can be used in conjunction with NDVI to correct NDVI in water impounded condition (Xiao *et al.* 2005; Xiao *et al.* 2006). Land surface wetness index (LSWI) is one of those index which takes both near-infrared (NIR) and shortwave infrared (SWIR) reflectance into the account to detect surface wetness (Chandrasekar *et al.*, 2010) and the vegetation water content (Jackson *et al.* 2004). Moreover, the strong short-wave infrared signal from flooded soil may drop significantly as growing rice canopy covers signals from the background soil. In order to estimate more accurate K_c of rice for crop water requirement from satellite data, these complex features of the paddy fields need to be analysed and should be considered for rice fields in various growing stages.

There are many polar orbiting satellites that provide continuous measurements of earth surface in red, NIR and SWIR wavelength region and support estimation of essential vegetation properties such as canopy cover, vegetation water content, biomass etc. Advanced

Wide field Sensor (AWiFS) of Indian Remote Sensing Satellite P6 (IRS P6) is one of these kind of versatile sensor that has capability to monitor crop canopy attributes at sufficiently optimal resolution due to its wide swath (740 km), moderate spatial resolution (56m) and high temporal resolution (05 days).

The real time water demand for rice-wheat system depends upon growth stages (phenological stage). It is possible to extract crop phenological stages from satellite image and estimate evapotranspiration from meteorological data with the satellite derived crop data. Keeping these points in view, the main objective of the study is the estimation of crop water requirement for rice-wheat cropping system from satellite data. To fulfill of main objective the following are the sub objectives: (i) To generate the cropping pattern map of the study area; (ii) To estimate the (near) real time spatially distributed crop coefficient for rice and wheat crops; and (iii) To estimate the crop water requirement based on crop coefficient approach for rice-wheat system.

2. Study area

Saharanpur district, Uttar Pradesh has tropical sub humid climate because of its proximity to Himalayan region and located between 29°34'45"N and 30°21'30"N latitude and 77°09'E and 78°14'45"E longitude. It belongs to the uppermost part of the Upper Ganga plain which is a sub-humid region between the dry Punjab plain and the humid middle Ganga plain within the monsoonal region of the Great Plains and naturally part takes the characteristics of the two adjoining regions. The average annual precipitation is 868 mm and most of the annual rain fall (about 90%) is received during the monsoon season (July to September). The average temperature recorded is 23.3°C. The highest percentage of humidity i.e. 72 to 85 per cent is found during the rainy season at the lower range of humidity between 29 to 51.5 per cent is recorded in the summers. The soil is mainly sandy and sandy loam, which is easily erodible by rain water and causing severe soil erosion. Thus the soils have high water absorbing and low water holding capacity. The most common crops grown in Saharanpur district are sugarcane, rice, wheat, maize, vegetables, fodder, mustard etc.

3. Methodology

3.1 ETo estimates from Penman-Monteith

The ET_o was computed by FAO Penman–Monteith method (Eq. 1) using meteorological data such as radiation, air temperature, air humidity and wind speed data (Allen *et al.* 1998). Weather data was collected from the meteorological observatory of Horticultural Experiment & Training Centre, Saharanpur. In FAO Penman-Monteith equation (Allen *et al.* 1998; Smith *et al.* 1996), a hypothetical grass reference surface is used to determine ET. It makes climate of particular region in different times of year a constant and reflects the potential demand of ET and so provides a standard to be related with the other crops.

From the original Penman-Monteith equation and the equations of the aerodynamic and surface resistance, the FAO Penman-Monteith method to estimate ET_o can be derived ET

$$ET_o = \frac{0.408\Delta(R_n - G) + \gamma \frac{900}{T + 273} U_2 (\theta_s - \theta_a)}{\Delta + \gamma(1 + 0.34U_2)} \text{ mm/day}$$

Where, E_{To} reference evapotranspiration [mm day^{-1}], R_n net radiation at the crop surface [$\text{MJ m}^{-2} \text{day}^{-1}$], G soil heat flux density [$\text{MJ m}^{-2} \text{day}^{-1}$], T mean daily air temperature at 2 m height [$^{\circ}\text{C}$], U_2 wind speed at 2 m height [m s^{-1}], e_s saturation vapour pressure [kPa], e_a actual vapour pressure [kPa], $e_s - e_a$ saturation vapour pressure deficit [kPa], Δ slope vapour pressure curve [$\text{kPa } ^{\circ}\text{C}^{-1}$] and γ psychrometric constant [$\text{kPa } ^{\circ}\text{C}^{-1}$].

By using the FAO Penman Monteith definition for E_{To} , one may calculate crop coefficients at research sites by relating the measured E_{Tc} with the calculated E_{To} .

3.2 Crop coefficient (Kc)

The crop coefficients are affected mainly by the crop characteristic, crop planting or sowing date, crop development rate, length of growing period and climate conditions. Depending on the time interval between wetting events, the magnitude of wetting event and the E_{To} the crop coefficient for initial growth stage $K_{c_{ini}}$ was interpolated from FAO-56 Fig. 30 (Allen *et al.* 1998) and typical values of crop coefficients for mid-season growth stage, $K_{c_{mid}}$ and late season $K_{c_{end}}$ are taken from FAO-56 Table 12 (Allen *et al.* 1998). Crop development takes place in four stages initial stage, crop development stage, mid season stage and late season stage (Doorenbos and Pruitt 1977). Monthly crop coefficient (Kc) was estimated using the guidelines given in irrigation and drainage paper FAO-56 (Allen *et al.* 1998) for rice and wheat crop depending upon the stage of growth. For specific adjustment in climates where minimum relative humidity (RH_{min}) differs from 45% or where wind velocity measured at 2 m height (u_2) is larger or smaller than 2.0 m s^{-1} , the Kc values at mid and end of season are adjusted as below:

FAO-Kc correction as per the local weather condition,

$$K_{c_{mid}} = K_{c_{mid}}(tab) + [0.04(u_2 - 2) - 0.004(RH_{min} - 45)] \left(\frac{h}{3}\right) 0.3 \quad (2)$$

$$K_{c_{end}} = K_{c_{end}}(tab) + [0.04(u_2 - 2) - 0.004(RH_{min} - 45)] \left(\frac{h}{3}\right) 0.3 \quad (3)$$

where, $K_{c_{mid}}(tab)$ and $K_{c_{end}}(tab)$ is the tabulated crop coefficient value for Kc from FAO 56 at mid and end stage, RH_{min} is the mean value for daily minimum relative humidity during the midseason growth stage (%), for $20\% \leq RH_{min} \leq 80\%$, and h is mean plant height during the mid-season stage (m) for $0.1 \text{ m} < h < 10 \text{ m}$.

The weather adjusted crop coefficient ($K_{c_{adj}}$) are linearly interpolated between the three growth stages (initial, mid and end) to have more numbers of $K_{c_{adj}}$ values.

3.3 Satellite data processing

In order to estimate evapotranspiration in Saharanpur district, the data used for the study includes multi-date (10 images) IRS P6- AWiFS of year 2009-10. The image contains four bands (green (0.52-0.59 μm), red (0.62-0.68 μm), near infrared (0.77-0.86 μm) and shortwave infrared (1.55-1.70 μm)) of spatial resolution (56m at nadir, 70m at field edge), radiometric resolution (10 bits) covering a swath of 740 km. In monsoon season it is very difficult to get optical data due to constant cloud cover. In this context IRS-P6 AWiFS data can play a major role in phenological study of rice crop. The satellite data used in study are mentioned in Table 1.

Table 1: AWiFS data used and corresponding growth stage for rice-wheat cropping system in study area

Crop	Growth stages	Satellite data procured
Rice	Transplanting	July 14, 2009
	Tillering	August 22, 2009
	Grain filling	October 08, 2009
	Maturity	October 28, 2009
Wheat	Crown root initiation	December 24, 2009
	Tillering	January 31, 2010
	Flowering	February, 2010
	Grain filling	March 16, 2010
	Maturity	April 04, 2010

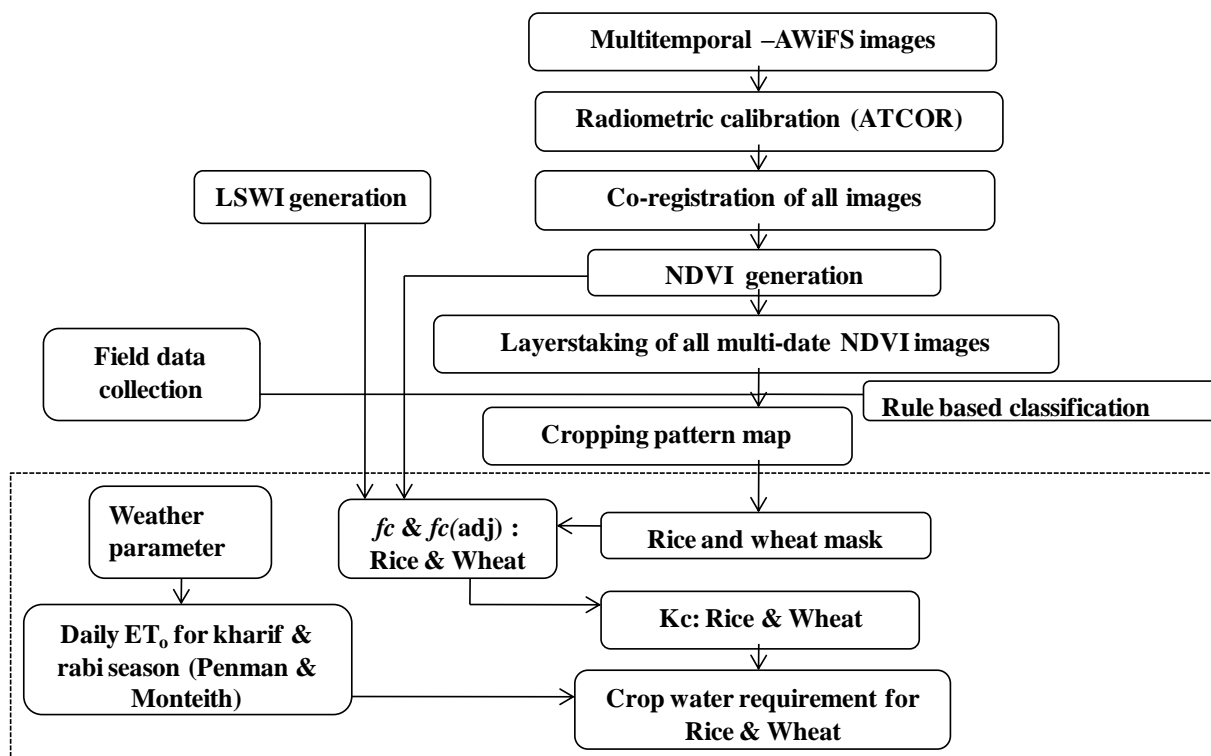


Figure 1: Flow chart of methodology

3.3.1 Atmospheric and geometric corrections

To compare multi-temporal satellite images with different times of acquisition, radiometric and atmospheric correction is an important image pre-processing step since it is needed to convert the at-satellite spectral radiances of satellite imagery to their at-surface counterparts. After time atmospheric correction, changes observed are due to different features on the earth's surface rather than differences of the atmospheric condition in order to bring all scenes to a common radiometric datum. In this work, radiometric correction was mainly done using

Atmospheric and Topographic Correction for Satellite Imagery (ATCOR) model to remove or reduce the influence of atmospheric and solar illumination.

All the images (10 in no.) were co-registered with each other to bring all images in the same geometric datum.

3.3.2 Computation of vegetation Indices (VIs)

Vegetation indices have been calculated using multi-temporal images from AWIFS sensor acquired during double crop growing season of year 2009-10. The NDVI as measure of fractional vegetation cover for each date of satellite image was calculated as:

$$NDVI = \frac{NIR - R}{NIR + R} \quad (4)$$

Where, NIR and R represents atmospherically corrected reflectance in red and near infrared region. NDVI values range from -1 to 1, extreme negative values represent water, values near to zero represent bare soil and values above 0.6 represent dense green vegetation.

A biophysical parameter, fractional canopy cover (f_c) derived from NDVI has been calculated as:

$$f_c = \left(\frac{NDVI_i - NDVI_{min}}{NDVI_{max} + NDVI_{min}} \right)^2 \quad (5)$$

Where, $NDVI_i$ is the NDVI value of particular pixel, $NDVI_{max}$ and $NDVI_{min}$ are maximum and minimum growing season NDVI value at 95% and 2% percentiles of pixels, respectively.

Similarly LSWI was derived from multi-temporal data in order to account for surface water ponding. LSWI for each date of image acquisition was estimated as:

$$LSWI = \frac{NIR - SWIR}{NIR + SWIR} \quad (6)$$

Where, NIR and SWIR are atmospherically corrected reflectance in NIR and SWIR region. Further LSWI images so derived were used in derivation of water stress scalar (W_s) (Xiao *et al.*, 2004):

$$W_s = \frac{1 - LSWI_i}{1 + LSWI_{max}} \quad (7)$$

Where, $LSWI_i$ is LSWI value of particular pixel, $LSWI_{max}$ is the maximum LSWI value of each pixel in growing season.

For rice we have derived a comprehensive index which includes W_s to develop regression equation with K_c while for wheat we have considered f_c only (W_s excluded) for relationship with K_c .

$$\text{For rice, Wetness adjusted } f_c = a \times W_s + b \times f_c \quad (8)$$

Where, wetness adjusted f_c ($f_c(\text{adj})$) was the comprehensive index for K_c estimation in rice, a & b are weights of W_s and f_c , respectively defined arbitrarily based on growth stage (varies between 0 to 1 and $a+b \leq 1$). Since impounded water background during transplanting stage affects spectral signature of rice plant, we might give more weight to W_s at the initial stage while at mid and end stage f_c can be given more weights.

3.3.3 Cropping pattern generation using rule based classifier

Cropping pattern is defined as spatial arrangement of crops in a given area. It is categorized on the basis of crop season as Kharif (June-October), Rabi (December-April). The cropping pattern map for year 2009-10 was generated by integration of temporal AWiFS NDVI of two season data. Layer stack multi-date NDVI images were classified by rule-based classification.

The analyzed multi-temporal NDVI images were used as a basis for the knowledge acquisition process for the rule-based classification.

3.4 Relationship of Kc and vegetation indices

The relationship between derived vegetation indices and interpolated Kc_{adj} of rice-wheat for corresponding months were developed. Crop coefficient maps were generated for each month of rice-wheat crop season by applying regression equation over the image in MODEL MAKER of Erdas Imagine. Monthly reference crop evapotranspiration (ET_o) was estimated based on FAO-56, Penman Monteith method. ET_o was combined with spatially distributed Kc maps of different months of wheat crop season to generate crop evapotranspiration (ET_c) maps of each month.

3.5 Calculation of irrigation water requirement for rice wheat system

In order to compute the crop water requirement (CWR), Kc values for the rice and wheat crop were estimated and multiplied with the potential evapotranspiration.

$$CWR = Kc \times ET_o \quad (9)$$

The crop water demand of rice and wheat were estimated using spatially distributed ET_c maps for months July, August, September, October 2009, and December, January, February, March, April 2010 respectively.

4. Results and discussion

4.1 Temporal profile of NDVI of various cropping system

Temporal profile of NDVI for various cropping systems identified in study area was extracted for dominating patches and shown in figure 2. Most of the sugarcane has been harvested in month December in sugarcane-wheat system while rice has been harvested in last week of October. This key point has differentiated these two systems very well. Moreover, in month of July NDVI value of sugarcane area is higher as compared to rice. In sugarcane system the NDVI value of rabi season is very low and helped in distinguishing it from sugarcane-wheat system.

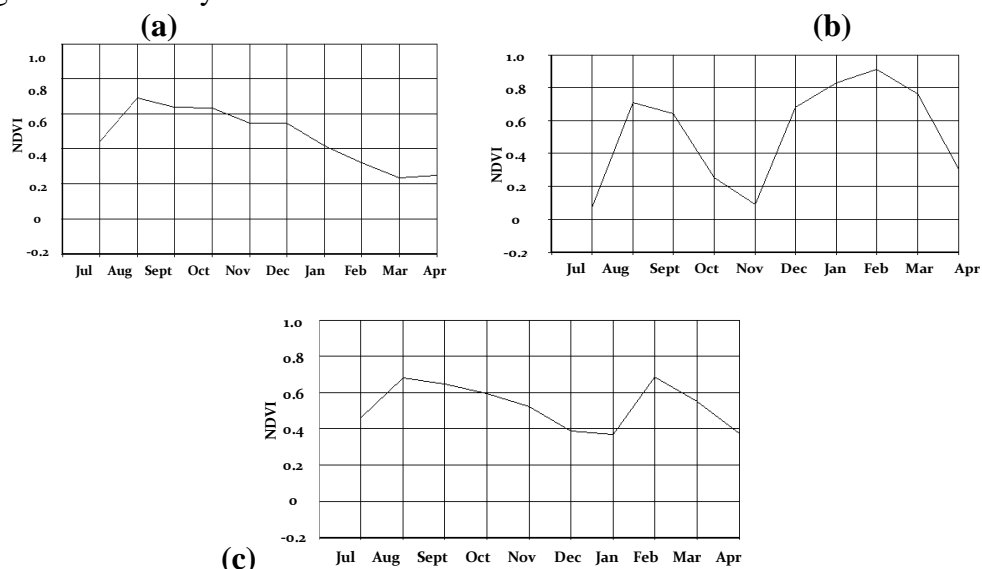


Figure 2: Temporal profile of NDVI of various cropping system in study area (a) Rice-wheat; (b) Sugarcane only and (c) Sugarcane-Wheat

4.2 Cropping pattern map using rule based classification technique

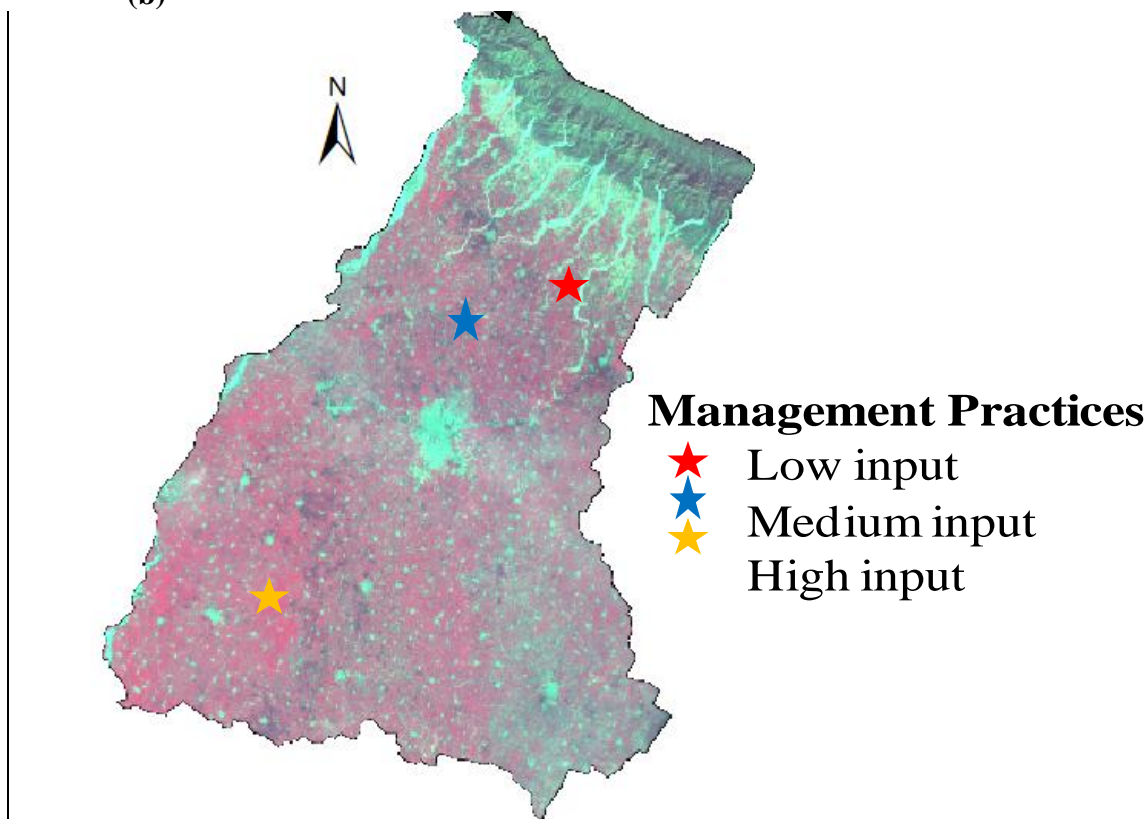
Different rules using temporal NDVI of ten images at different growth stages have been generated to distinguish the various cropping system (Fig. 3) in the study area. The accuracy of classification was assessed by ground truth samples and confusion matrix is created. Confusion Matrix showed the accuracy of a classification result by comparing a classification result with ground truth information. The knowledge-based classifier has shown high classification accuracy for all cropping system as small field size of crops prevailing in study area. The overall accuracy of classification was found to be 85.3% and the kappa value was 0.82 for the cropping season. The user's and producer's accuracy of rice-wheat cropping system were 81.2% and 90% respectively. From the classified image area under rice-wheat cropping system was found out to be 45711 ha (24.2% of net sown area) given in table 2.

Table 2: Cropping pattern area extracted from satellite image for year 2009-10 of Saharanpur district

Cropping system	Area (ha)	% Area
Rice-Wheat	45711.07	24.2
Sugarcane	84021.91	44.6
Sugarcane-Wheat	52302.21	27.7
Maize -Fallow	3207.81	1.7
Maize-Mustard	1572.70	0.83
Fallow-Fodder	1495.24	0.8

(a)

(b)



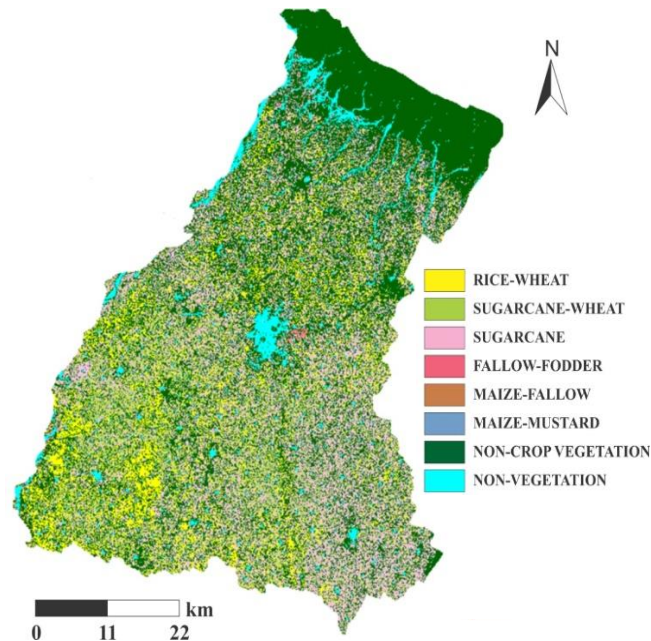
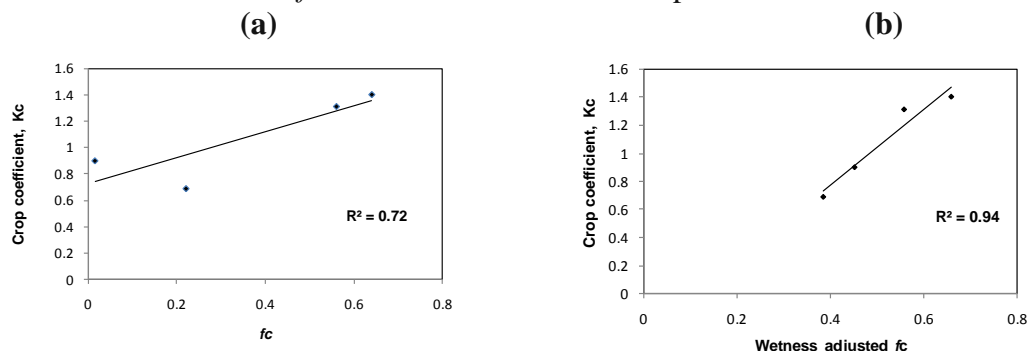


Figure 3: (a) False colour composite of Study area (February, 2010) (b) Cropping pattern map of Saharanpur district using rule based classification technique

4.3 Development of relationship of Kc with f_c (adj) (for rice) and f_c (for wheat)

In rice season, NDVI value was very less at initial stage due to stagnant water in paddy field, so, calculated fractional canopy cover, f_c was also very less while tabulated Kc FAO value was high. To adjust f_c as per the initial stage of paddy we have used LSWI, an indicator of flooding. The biophysical parameters (wetness adjusted fractional canopy cover, $f_c(\text{adj})$ and fractional canopy cover, f_c) derived by NDVI and LSWI for rice and NDVI alone for wheat were correlated with the crop coefficients Kc FAO (Kc ini, Kc mid and Kc end) to develop regression equations. The Kc ini, Kcmid and Kc end values for rice and wheat crop obtained from FAO-56 and adjusted for local conditions were 0.9, 1.4 and 0.69 and 0.3, 1.14 and 0.34 respectively. The Kc values within the crop growth stages were linearly interpolated.

The pixel values of $f_c(\text{adj})$ and f_c by 3×3 window of a rice and wheat respectively were extracted for each satellite pass to produce crop-specific Kc FAO (corrected for local conditions and interpolated) curves for the growing season. The regression equations were developed by correlating $f_c(\text{adj})$ and f_c with all the weather adjusted Kc FAO values for rice and wheat crop respectively as shown in Figure 4. Figure 4(a) shows moderate correlation between rice Kc FAO (corrected for local conditions and interpolated) and f_c without wetness correction especially at initial stage with coefficient of determination r^2 of 0.72. After wetness correction in rice by W_s the $f_c(\text{adj})$ with Kc FAO showed improved positive relationship with excellent r^2 of 0.94 as shown in Fig. 4(b). Figure 4(c) also demonstrated strong Positive correlation of f_c with Kc FAO of wheat crop with r^2 values 0.91.



(c)

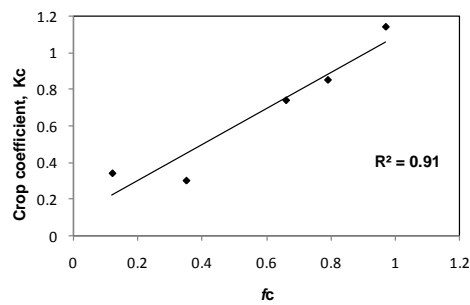


Figure 4: Relationship of crop coefficients Kc with (a) f_c^* (for rice crop) (b) $f_c(\text{adj})^{**}$ (for rice crop) and (c) f_c^{**} (for wheat crop) values

* f_c is calculated by NDVI values only

** $f_c(\text{adj})$ is calculated by NDVI and LSWI values

4.5 Monthly crop coefficient and crop water requirement estimation of rice and wheat crop

Monthly crop coefficient was mapped at pixel resolution by applying regression equations developed for $f_c(\text{adj})$ and f_c with Kc FAO (corrected for local conditions and interpolated) in Spatial Modeler module of ERDAS IMAGINE. The output of the model represents the spatially distributed crop coefficient maps with pixel-wise Kc values, as presented in Figure 5. The Figure 6 shows that the Kc (based on $f_c(\text{adj})$) values of rice crop varied from <0.2 to 0.5, 0.8 to 1.6, 0.6 to 1.4 and <0.4 to 1.0 for different months of monsoon season July, August, September and October respectively.

The figure 6 illustrates that the Kc (based on f_c) values of wheat crop varied from <0.2 to 0.5, 0.5 to 0.9, 0.5 to 1.3, 0.5 to 1.3 and <0.3 to 0.7 for different months of winter season December, January, February, March and April respectively. The Kc values are spatially distributed, which represent different conditions and different crop growth stages due to different sowing dates.

The remote sensing derived Kc also explains the effect of management practices (Allen *et al.*, 1998) prevailing in study area as shown in Figure 6. The management practices information was collected by Farmer's interview during ground truth data collection and on the basis of this management practices in area were divided into three categories (Fig. 3(a)). High input represents more frequency of irrigation water application (3.0-4.0) along with high fertilizer application for wheat crop as compared to medium (irrigation frequency of 2.0-3.0) and low (irrigation frequency of 0-2.0) input. Figure 6 clearly indicates the spatial variability in predicted Kc caused by varied management practices. Across study area, higher magnitude of Kc values was noticed where optimum or higher management input viz., irrigation and fertilizer applications practiced. In general, foot hills of Shivalik and piedmont plains with coarse textured soils had low input applications and thus had lower Kc values.

The output of pixel-wise Kc map was multiplied with computed reference evapotranspiration (ET_o) using Eq. 9 for corresponding months in software MODEL MAKER of ERDAS IMAGINE to generate the ET_c maps. The spatially distributed Kc FAO (based on $f_c(\text{adj})$ and f_c) of rice and wheat crop so obtained has led to derive the spatially distributed ET_c values for different months of kharif and rabi crop season respectively.

Monthly averaged crop water demand based on ETC of rice and wheat crop is presented in Table 3. The volume of crop water demand based on ETC of kharif (July, August, September and October months) season, 2009 and rabi (December, January, February, March and April) season, 2010 were estimated 241.66, 531.34, 440.86 and 192.63 Mha.m and 127.43, 135.77, 305.55, 262.84 and 204.50 Mha.m respectively. It shows that ETC demands for the rice and wheat crop are low in the month of July, 2009 and December, 2009 (initial growth stage of rice and wheat respectively), maximum in month of August, 2009 and February, 2010 and reduced in later months as the crop is approaching to its maturity in rice and wheat crop growth cycle respectively.

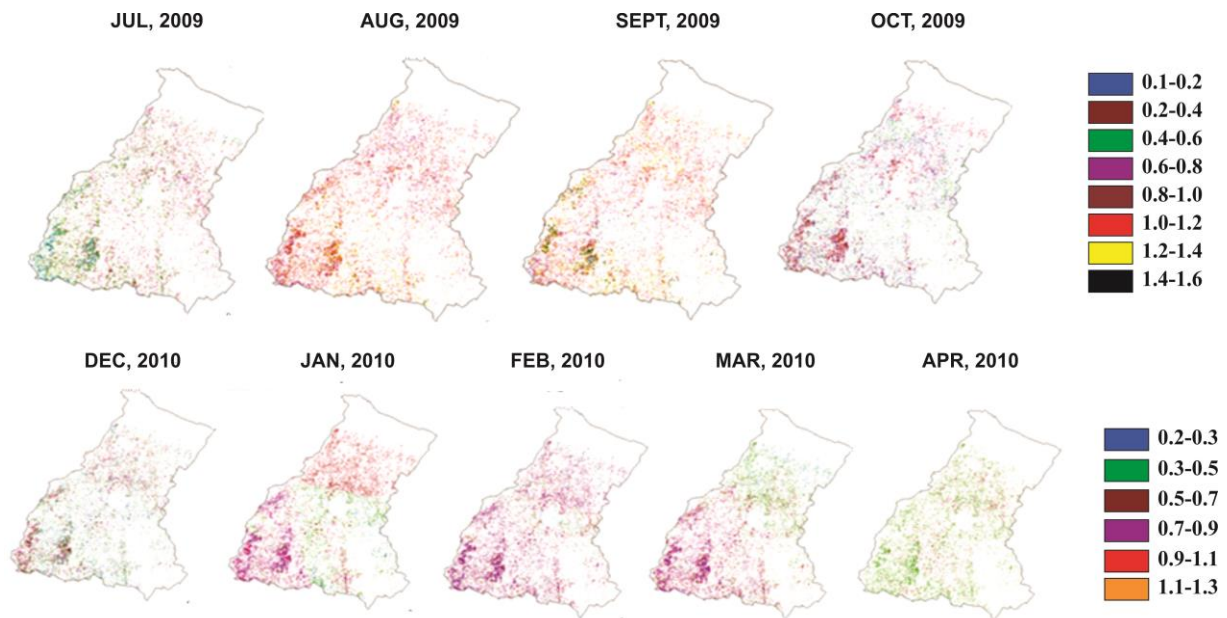


Figure 5: Monthly spatially distributed crop coefficient (Kc FAO) maps generated using wetness adjusted f_c values and f_c of rice and wheat crop

Table 3: Month wise crop water demand based on actual crop evapotranspiration (ETC) using Kc FAO (wetness adjusted f_c values and f_c) for rice and wheat crop in Saharanpur district

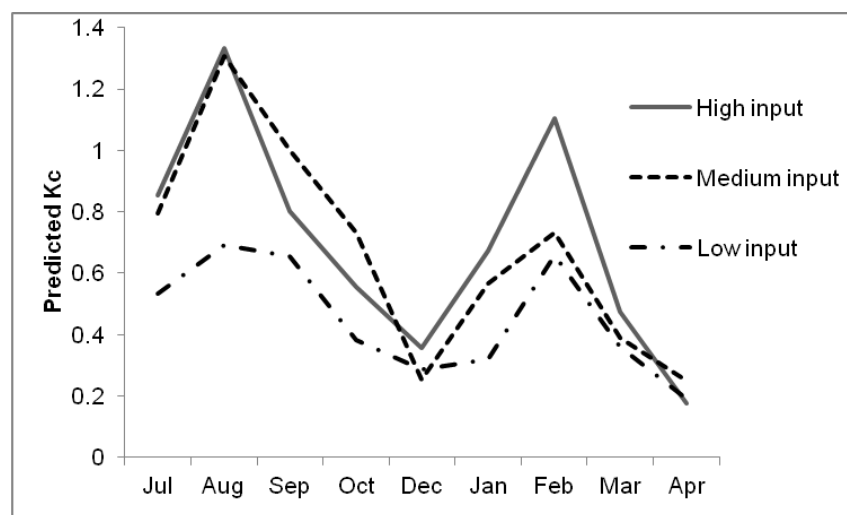


Figure 6: Graph showing variation of predicted Kc as per the management practices in study for rice-wheat system

5. Conclusions

The present study explores mapping of spatially distributed crop water requirement in rice-wheat system by wetness corrected Kc derived from multi-temporal AWIFS data. The regression based models have been developed by derived vegetation indices (fc_{adj} & fc) from NDVI & LSWI and weather adjusted Kc of rice & wheat crop for corresponding months have generated spatially distributed actual crop evapotranspiration. The crop coefficients based on wetness adjusted fc has shown reasonably accurate both temporal and spatial pattern of Kc and consequently crop water demand for rice crop. The satellite derived Kc has shown the effect of management practices and so superiority over using tabulated FAO Kc. Therefore, the information generated can be used to supply appropriate amount of irrigation water at different locations of study area as per the actual crop water demand to prevent the environmental problems.

6. References

1. Allen, R.G., Pereira, L.S., Raes, D., Smith, M., (1998), Crop evapotranspiration: guidelines for computing crop water requirements, FAO Irrigation and Drainage Paper 56, FAO, Rome, Italy.
2. Allen, R.G., (2000), Using the FAO-56 dual crop coefficient method over an irrigated region as part of an evapotranspiration intercomparison study, *Journal of Hydrology*, 229, pp 27–41.
3. Baret, F., Guyot, G., (1991), Potentials and limits of vegetation indices for LAI and APAR assessment, *Remote Sensing of Environment*, 35, pp 161–173.
4. Bastiaanssen, W.G.M., Molden, D.J. and Makin, I.W., (2000), Remote sensing for irrigated agriculture: examples from research and possible applications, *Agricultural Water Management*, 46(2), pp 137–155.
5. Bausch, W.C., Neale, C.M.U., (1987), “Crop coefficients derived from reflected canopy radiation: A concept. *Trans. ASAE.*”, 30(3), pp 703–709.
6. Bausch, W.C., (1995), Remote sensing of crop coefficients for improving the irrigation scheduling of corn. *Agric. Water Manage.*, 27, pp 55–68.
7. Carlson, T.N., Ripley, D.A., (1997), On the relation between NDVI, vegetation cover and leaf area index. *Remote Sensing of Environment*, 62, pp 241–252.
8. Chandrasekar, K., Sessa Sai, M.V.R., Roy, P.S., Dwevedi, R.S. (2010), Land Surface Water Index (LSWI) response to rainfall and NDVI using the MODIS Vegetation Index product, *International Journal of Remote Sensing*, 31(15), pp 3987–4005.
9. Choudhury, B.J., Ahmed, N.U., Idso, S.B., Reginato, R.J., Daughtry, C.S.T, (1994), Relations between evaporation coefficients and vegetation indices studied by model simulations, *Remote Sensing of Environment*, 50, pp 1–17.

10. Doorenbos, J. and Pruitt, W.O., (1977), Guidelines for predicting crop water requirements. FAO Irrigation and Drainage Paper No 24, FAO, Rome, Italy.
11. Duchemin, B., Goubier, J., Courier, G., (1999), Monitoring phenological key-stages and cycle duration of temperate deciduous forest ecosystems with NOAA-AVHRR data, *Remote Sensing of Environment*, 67, pp 51–67.
12. Duchemin, B., Frappart, F., Maisongrande, P., Magnac, M., Mougenot, B., Chehbouni, A., Dedieu, G., (2002), Water budget with phenology derived from optical satellite data. In: *Proceedings of the First International Symposium of Recent Advances in Quantitative Remote Sensing*, Valencia, Spain, 16–20 September.
13. Eitzinger J, Marinkovic D, Hořsch J., (2002), Sensitivity of different evapotranspiration calculation methods in different crop-weather models. In: Rizzoli, A.E., Jakeman, A.J. (Eds.), *Integrated Assessment and Decision Support. Proceedings of the First Biennial Meeting of the International Environmental Modelling and Software Society (IEMSS)*, Lugano, Switzerland, 24–27 June, 2: 395–400.
14. Evett, S.R., Howell, T.A., Schneider, A.D., Tolk, J.A., (1995), Crop coefficient based evapotranspiration estimates compared with mechanistic model results. In: Espey, W.H., Combs, P.G. (Eds.), *Water Resources Engineering, Proceedings of the First International Conference*, vol. 2, San Antonio, TX, USA, 14–18 August.
15. Gutman, G.G., (1999), on the use of long-term global data of land reflectances and vegetation indices derived from the advanced very high resolution radiometer, *Journal of Geophysical Research*, 104, pp 6241–6255.
16. Hall, F.G., Townshend, J.R., Engmann, E.T., (1995), Status of remote sensing algorithms for estimation of land surface parameters, *Remote Sensing of Environment*, 51, pp 138–156.
17. Heilman, J.L., Heilman, W.E., Moore, D.G., (1982), Evaluating the crop coefficient using spectral reflectance, *Agronomy Journal*, 74, pp 967–971.
18. Huete, A.R., (1988), A soil-adjusted vegetation index (SAVI), *Remote Sensing of Environment*, 25, pp 295–309.
19. Jackson, R.D., Idso, S.B., Reginato, R.J., Pinter, P.J. Jr., (1980), Remotely sensed crop temperatures and reflectances as inputs to irrigation scheduling. In: *Proceedings of the Special Conference on Irrigation and Drainage*, Boise, Idaho. ASCE, New York, 23–25 July, pp 390–397.
20. Jackson, R.D., Huete, A.R., (1992). Interpreting vegetation indices, *Prev. Vet. Med.* 11, pp 185–200.
21. Jensen, M.E., Burman, R.D., Allen, R.G., (1990), Evapotranspiration and irrigation water requirement, *ASCE Manuals and Reports on Engineering Practice No. 70*, 332.
22. Kite, G.W., Droogers, P., (2000), Comparing evapotranspiration estimates from satellites, hydrological models and field data, *Journal of Hydrology*, 209, pp 3–18.

23. Mishra, P., Tiwari, K.N., Chowdary, V.M., Gontia, N.K., (2005), Irrigation water demand and supply analysis in the command area using remote sensing and GIS, *Hydrology Journal IAHR.*, 28(1–2), pp 59–69.
24. Moran, M.S., Mass, S.J., Pinter, P. J. Jr., (1995), Combining remote sensing and modelling for estimating surface evaporation and biomass production, *Remote Sensing Rev.*, 12, pp 335–353.
25. Myneni, R.B., Keeling, C.D., Tucker, C.J., Asrar, G., Nemani, R.R., (1997), Increased plant growth in the northern high latitudes 1981 to 1991, *Nature.*, 386, pp 698–702.
26. Patel, N.R., Rakhesh, D., Mohammed, A.J., (2006), Mapping of Regional evapotranspiration in Wheat using Terra/MODIS satellite data, *IAHS Hydrological Sciences Journal*, 51(2), pp 325-333.
27. Ray, S.S., Dadhwal, V.K., (2001), Estimation of crop evapotranspiration of irrigation command area using remote sensing and GIS, *Agricultural Water Management*, 49, pp 239–249.
28. Rouse, J.W., Haas, R.H., Schell, J.A., Deering, D.W., Harlan, J.C., (1974), Monitoring the vernal advancement and retrogradation of natural vegetation, NASA/GSFC, Type III, Final Report, Greenbelt, MD, 1–371.
29. Smith, M., Allen, R.G., Pereira, L.S., Camp, C.R., Sadler, E.J., Yoder, R.E., (1996). Revised FAO methodology for crop water requirements. Proc of the international conference on evapotranspiration and irrigation scheduling, San Antonio, Texas, USA, 3–6 Nov 1996, 116–123.
30. Snyder, R.L., Lanini, B.J., Shaw, D.A., Pruit, W.O., (1987), University of California. Division of Agricultural and Natural Resources Leaflet 21427, 12.
31. Xiao, X., Boles, S., Liu, J., Zhuang, D., Frohking, S., Li, C., Salas, W., Moore, III B, (2005), Mapping paddy rice agriculture in southern China using multi-temporal MODIS images, *Remote Sensing of Environment*, 95, pp 480-492.
32. Xiao, X., Boles, S., Frohking, S., Li, C., Babu, J.Y., Salas, W., Moore, III B, (2006), Mapping paddy rice agriculture in South and Southeast Asia using multi-temporal MODIS images, *Remote Sensing of Environment*, 100, pp 95–113.